Texas Tech University
2006 Sandia MEMS Design Competition
Module 2

Mahmood Subhani, Jay Friend, Zach Jernigan, Stephanie Walters, Ganapathy Sivakumar, Mark Tabije, John Lusk, Jennifer Onita, Morshed Khandaker, Brian Bowden, Avinash Madadi, Paul Bowling, Najib Nawas, Mark Sapp, Chris Mills, John Allison, and T. Dallas

Texas Tech University, Lubbock, TX

CONTENTS

ABSTRACT
1. DESIGNS
A. MEMS Monorail
B. Tensile testing of Polysilicon Specimens
C. Bend Testing of Polysilicon Specimens
D. Mechanical Characterization of Bio-cell
2. NOTES

Abstract

We describe here Texas Tech University's module for Sandia National Laboratories' 2006 SUMMiT V MEMS Design Competition – Characterization/Reliability/ Materials & Surface Science category. The module contains an actuator system to test friction (Monorail) and numerous stress inducing systems for testing polysilicon structures and biological systems. The work has been generated through TTU's MEMS Courses and the 2005 MEMS Summer Institute at TTU.

1. DESIGNS

A. MEMS Monorail

The MEMS Monorail is a dynamic system designed to allow motion of microscopic cars along a track. Specifically, the system will be used to analyze the friction and stiction of 2-dimensional bearings and wear on dimples as the car goes through it's rainge of motion. Applications for the MEMS Monorail include a MEMS conveyor system or assembly line with a micro-gripper placed somewhere on the line to add and remove items from the conveyor. The current system consists of two (2) cars, the rails, and the drive system which includes a gear, gear arm, and TRA.

The rails are the key part of this system which keeps the platform from moving off the track. The rails consist of a poly 3 extension which hangs over the poly 1 and 2 layers by 10 µm. This extension prevents the platform from moving above the poly 3 layer. Also on the rails, there are multiple SaxOx 1 and SaxOx 3 cuts which allows for more adhesion to the die while maintaining the normal vertical height of the layers. The track bends to show the turning capability of the platforms and the swivel pin system. The turn is 30° from the start to the middle of the turn. The main constraint on the maximum turning radius is ensuring the carts will line up horizontally on the track after the turn. Currently, the rails are about 1085 µm long and the widths of the rails are 130 µm on the poly 3 level and 120 µm on the poly 1/2 layer.

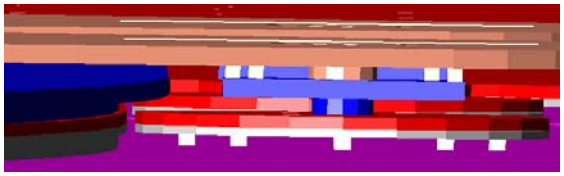

Figure A1: The 2-dimensional bearings which help move the platform along the rails. The 1 µm gap from the rail and bearing can be seen as well as the dimples which keep the bearing at the polysilicon's allotted vertical height.

The cars are constrained to follow the track through two, free rotating bearings. These two bearings keep the monorail horizontally aligned to the rails.

The bearings are designed to be about 1 µm away from the rails. A swiveling pin hitch system is located at the rear of the car.

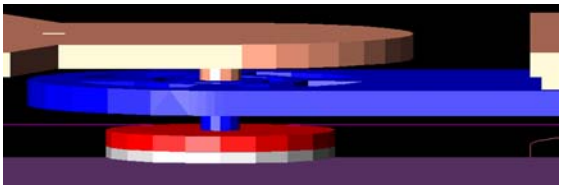

Figure A2: The swivel pin hitch system which allows the cars to turn on the track freely. The swivel pin hitch system also has four (4) support arms on the poly 3 layer which keeps the end car from moving to close or far from the beginning car.

This pin is designed to allow the front car to go into the turn while the rear of the car is still in the straight-away. The pin consists of a cap on the poly 2 and 4 layers. Inside, a pin runs from the poly 2 and 4 cap through a hole slightly larger then the pin in poly 3.

The drive system consists of a standard low-voltage TRA, gear, and gear arm that attaches to the rear hitch of the last car.

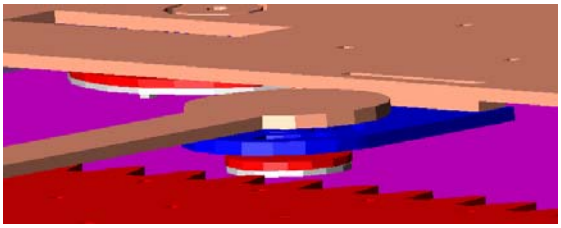

Figure A.3 The figure shows the gear arm attached to the hitch of the last car. There is not a cut in the poly 4 layer like the poly 3 layer because ensures that more force is applied when moving the cars forward.

The size of the gear determines how fast the platforms will travel. The gear arm is attached to the gear by a pin that protrudes upwards extending to the poly 4 level. On the poly 4 layer, there is a cap which prevents the gear arm from going higher then this level. The gear arm has to be on the poly 4 layer because if it was on any other level, when the car was in motion on the track, the gear arm would interfere with the rail.

The MEMS Monorail is actuated when a voltage is applied to the TRA. When this voltage is applied the TRA will turn the gear which is composed of 202 teeth and has the gear arm attached.

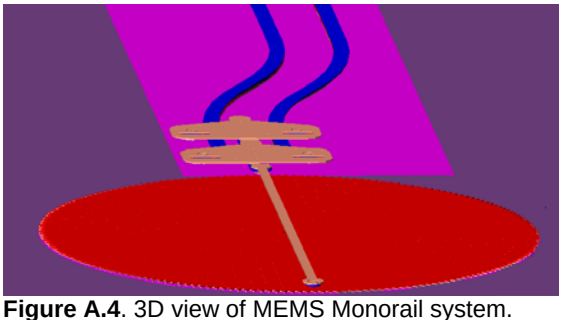

Figure A.4. 3D view of MEMS Monorail system.

As the gear is moved in a circular direction, the gear arm will push or pull, depending on the location of the gear arm, the platforms along the test track allowing the free spinning bearings to turn when contact is made with the bearings and the track. This motion can be better illustrate when looking at Figure A.4 showing the entire system. The platforms will be moved a total of 800 µm. The entire system is about 2 mm by 1.5 mm.

The MEMS Monorail is a great educational tool for various age levels. For kids, they will be able to associate the size of a normal train system to the size of the MEMS systems. Plus, children will be able to understand all the components which are used to make the monorail system work. Teenagers will be able to start to grasp the concept and usage of the multiple polysilicon layers and the SUMMiT V process. Adults will appreciate the complexity of the two dimensional free spinning bearings along with the hitch system which allows the platforms as a whole to turn. People of all ages will be intrigued by new and different ways to design tracks for a monorail system

B. TENSILE TESTING OF POLYSILICON SPECIMENS

Objectives:

The objective of this study is to design an *in situ* tensile test device to characterize the mechanical properties of a polysilicon specimen. The device is built using three different types of tensile specimens: (1) bow tie specimen, (2) Single edge notch tensile (SENT) specimen and (3) Double edge notch tensile (DENT) specimen. The scope of work is twofold: Firstly, design of an actuator in SUMMIT V to produce breaking force for these specimen and secondly, measure tensile and fracture toughness, Young's modulus and Poison's ratio of polysilicon.

Test device configuration:

The test device consists of three components: (1) an array of electro-thermal actuators, (2) connecting beam, and (3) a tensile specimen. These integrated actuators are connected to the one end of a tensile specimen through a suspended beam, while the other end of the specimen is anchored to the substrate. Bow tie tensile specimen will be used to find the yield properties (tensile strength, Young modulus and Poisson's ratio) of polysilicon, whereas, edge notch specimens were used to find fracture property (fracture toughness).

Working Principle:

This actuator works by the hot arm-cold arm principle. When a voltage is applied across the hot arm of the actuator, it experiences a thermal expansion in the direction away from the cold arm. This pulling force creates tension in the tensile specimen placed between anchor and connecting beam. Deformation at each load step and breaking force of the specimen due to actuating force can be measured directly by optical methods of interferometric microscope.

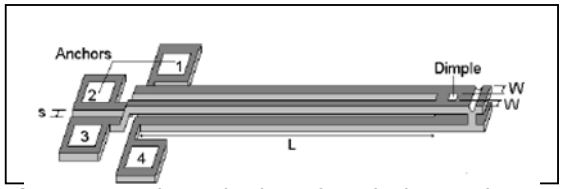

Figure B.1 Schematic view of Vertical-Lateral thermal actuator [Shannon Zelinski].

Device Design:
The electro-thermal actuators, as shown in Figure B.1, were considered for our design due to their capability of producing higher actuation force than electrostatic comb drive. To find out yield properties (tensile strength, Young's modulus and Poison's ratio) of polysilicon, a thermal actuator was designed to create the failure force, F_c and deformation, δ_c of the bow tie tensile specimens [1] as shown in .

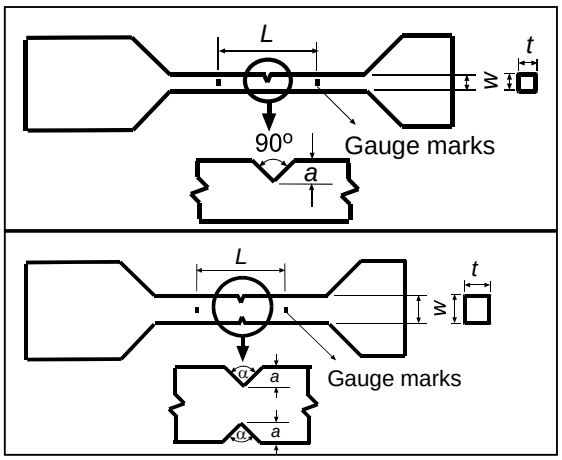

Figure B.3 Schematic view micro-specimen: (a) SENT (b) DENT.

The failure force and critical deformation before fracture were determined by the following expressions. The value of critical fracture toughness and Young modulus of polysilicon, assumed for these calculations, were 0.7 MPam$^{1/2}$ [**3**]and 169 GPa, respectively.

$$F_c = \frac{4 \times K_{IC} \times tw^2}{3 \times L \times \sqrt{\pi a} \times f\left(a/w\right)} \qquad (3)$$

and

$$\delta_c = \frac{F_c \times L^3}{16 \times E \times t \times w^3} \qquad (4)$$

Analytical models:
Tensile strength
A graph of the applied stress or actuation forces versus strains or the changes in the length as shown in **Error! Reference source not found.** will be plotted to find tensile strength [**4**]and spring constant of polysilicon. The break or rapture point of the specimen will be found by accounting the rapture load.

Young Modulus

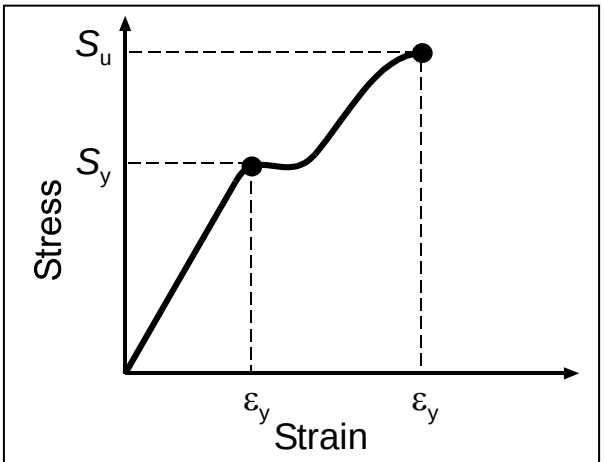

Figure B.4 Actuation force vs. gauge length deformation of bow tie specimen.

Young modulus of polysilicon can be found by following expression:

$$E = \frac{F}{w \times t \times \varepsilon} \qquad (5)$$

where ε is the normal strain. This value can by found by measuring the change in the gauge length, δ, (marked by distance between two pointers) due to the actuation force, *F*. The expression of normal strain is:

$$\varepsilon = \frac{\delta}{L} \qquad (6)$$

Interferometric microscope will be used to note the change in gauge length with precision. The actuation force due the applied current can be found by the following equation:

$$F = \frac{4\alpha\rho E}{\kappa} I^2 \qquad (7)$$

where *I* is the applied current. The values of thermophysical properties like coefficient of thermal expansion, α, resistivity, ρ,thermal conductivity, κ and Young modulus, *E,* of polysilicon can be found from literature [**5**].

Poisson's ratio
Poisson's ratio can be found using the following equation:

$$\nu = \frac{\varepsilon_L}{\varepsilon} \qquad (8)$$

where ε_L is the lateral strain. This value can by found by measuring the change in the width of gauge section, δ_L, due to the actuation force, *F*. The expression of normal strain is:

$$\varepsilon_L = \frac{\delta_L}{w} \qquad (9)$$

Fracture property

The fracture toughness of the notch specimens can be found by measuring the fracture load. This load causes propagation of a crack at the tip of the SENT or DENT specimen. The fracture toughness can be found using the following expression [**6**]:

$$K_{IC} = \sigma_{\max}\sqrt{\pi a}\, f\left(a/w\right) \qquad (10)$$

where σ_{max} is the maximum stress at the notch tip due to fracture load. In Eq. (10), the shape function, *f*(*a/w*), can be found from literature. The maximum stress due to fracture load can be found by the following expression:

$$\sigma_{\max} = \frac{F}{w \times t} \qquad (11)$$

SUMMiT V model

The geometric dimension used to model the bow tie tensile specimen is shown in

Table 1. To implement the tensile strength characterization in SUMMiT V, we use the design as shown in the figure B.5. The actuators are designed on poly 1, 2 and 3 layers. The fixed end of these actuators is anchored to the substrate. A dimple cut is provided at the free end to avoid the snapping down of the actuator. The force generated is transferred to the specimen through a central beam on poly 4, which is connected to the movable end of the specimen, while the specimen is anchored at the other end to the substrate.

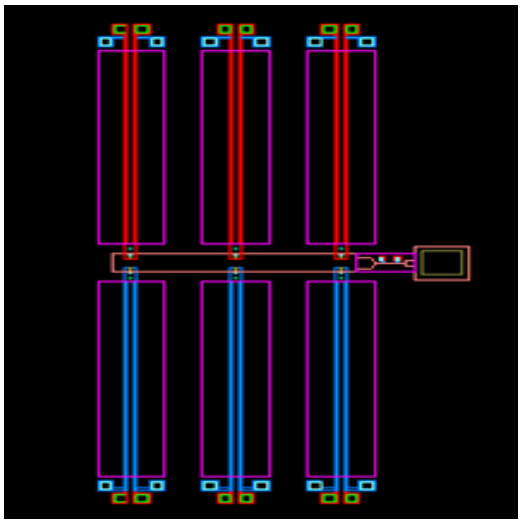

Figure B.5 SUMMIT V model for tensile test device.

Table 1 Geometric dimension of bow tie specimen

Geometric Dimension		Values (μm)
Gauge Length, *L*	=	10 mm
Width in the gauge section, *w*	=	1 mm
Thickness in the gauge section, *t*	=	2.25 mm

Table 2 Geometric dimension of SENT specimen

Geometric Dimension		Values (μm)
Gauge Length, *L*	=	10
Width in the gauge section, *w*	=	2
Thickness in the gauge section, *t*	=	2.25
Crack Length	=	1

Table 3 Geometric dimension of DENT specimen

Geometric Dimension		Values (μm)
Gauge Length, *L*	=	10
Width in the gauge section, *w*	=	4.8
Thickness in the gauge section, *t*	=	2.25
Crack Length	=	1

Expected Results:

Yield Property:

Table 4 Approximate analytical results for bow tie microspecimen

Tensile Strength	Required actuation Force, N	Young Modulus	Deflection (μm)
σ_c	F_c	E	δ
1.23E+09	2.77E-03	1.69E+11	7.28E-08

Fracture Property

Table 5 Approximate analytical results for SENT microspecimen

Fracture Strength	Required Actuation Force, *N*	Young Modulus	Deflection (μm)
K_{IC}	F_c	E	δ
7.00E+05	8.59E-04	1.69E+11	4.23E-08

Table 6 Approximate analytical results for DENT microspecimen

Fracture Strength	Required Actuation Force, N	Young Modulus	Deflection(μm)
K_{IC}	F_c	E	δ
7.00E+05	4.95E-03	1.69E+11	4.23E-08

Applications

1. This *in situ* test configuration can be used to measure yield and fracture mechanical properties of polysilicon.

2. Failure forces for the specimen can be achievable with the help of the designed actuator.

REFERENCES:

[1] **Allameh, S.M.** An introduction to mechanical-properties-related issues in mems structures. *Journal of Materials Science*, 2003, **38**(20), 4115-4123.

[2] **Bagdahn, J., Schischka, J., Petzold, M. and Sharpe Jr., W.N.** Fracture toughness and fatigue investigations of polycrystalline silicon. In *Reliability, Testing, and Characterization of MEMS/MOEMS, Oct 22-24 2001*, San Francisco, CA, United States, 2001, pp. 159-168 (The International Society for Optical Engineering).

[3] **Lee, S.H., Kim, J.S., Evans, J.W., Son, D., Pak, Y.E., Jeon, J.U. and Kwon, D.** Evaluation of microfracture toughness and microcracking with notch tip radius of si film structure for microactuator in hard disk drives. *Microsystem Technologies*, 2001, **7**(3), 91-98.

[4] Haque, M.A. and Saif, M.T.A. Microscale materials testing using mems actuators. *J. Microelectromech. Syst.*, 2001, **10**(1), 146-152.

[5] **Mankame, N.D. and Ananthasuresh, G.K.** Comprehensive thermal modelling and characterization of an electro-thermal-compliant microactuator. *J. Micromech. Microeng.*, 2001, **11**(5), 452-462.

[6] **Gomez, F.J. and Elices, M.** A fracture criterion for blunted v-notched samples. *Int. J. Fracture*, 2004, **127**(3), 239-264.

[5] **Mankame, N.D. and Ananthasuresh, G.K.** Comprehensive thermal modelling and characterization of an electro-thermal-compliant microactuator. *J. Micromech. Microeng.*, 2001, **11**(5), 452-462.

[6] **Gomez, F.J. and Elices, M.** A fracture criterion for blunted v-notched samples. *Int. J. Fracture*, 2004, **127**(3), 239-264.

C.BENDING TEST OF NOTCHED POLYSILICON SPECIMEN

Objectives:

The objective of this study is to design an *in situ* bending test device to find fracture strength of different kinds of bend specimens. The scope of work is twofold: Firstly, design of an actuator in SUMMIT V to produce maximum bending stress at the notch tip and secondly, measure fracture toughness of polysilicon for the bend specimens.

Test device configuration:

The test device consists of three components: (1) an array of bent beam actuators, (2) connecting beam, and (3) a bend specimen. The sole purpose of this test structure is to measure fracture toughness of three different kinds of notched bend specimens: (1) double-clamped specimen with V-edge notch at the center of the specimen [1], (2) V-shape [**2**], and (3) U-shape edge notch [**3**] near the fixed end of the specimen. For the first specimen, actuation force is applied on the opposite edge of the V notch, whereas, for the second and third specimen, force is acting at the other end of the specimen. Multiple actuators apply the required actuation to the bend specimen through a trunk, while the end of the specimen is anchored to the substrate. In all cases, the maximum bending stress occurs at the notch tip.

Working Principle

This thermal actuator works using the hot arm - cold arm principal. Two kinds of thermal actuators was used, namely, bent beam [4-6] and thermal actuator [7]. In bent beam actuator, voltage is applied across a set of slanted beams through anchor. The difference in thermal expansion between hot (slanted beam) and cold arm (trunk) results in a displacement of the trunk. In thermal actuator, voltage is applied across the hot arm of the actuator through hot and cold arm anchors as shown in Figure C.1 (b), it experiences a thermal expansion in the direction away from the cold arm. The resultant

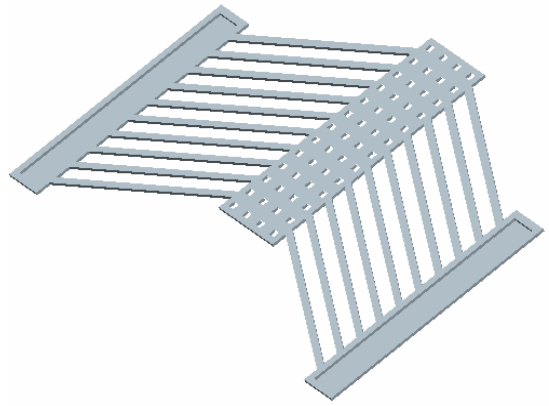

Figure C.1 (a) Solid model of the thermal bent beam actuator

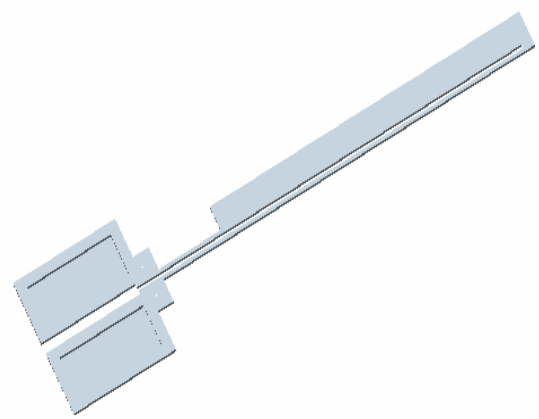

Figure C.1 (b) Solid model of hot-arm cold-arm actuator.

Movement of the thermal actuators pulls the bend specimen through trunk. This pulling force of trunk creates maximum bending stress at the notch tip of the bend specimens. The end of the bend specimens is anchored with the substrate. Deformation at each load step and breaking force of the specimen due to

actuating force can be measured directly by optical methods of interferometric microscope.

Device Design:

The electro-thermal actuators were considered for our design due to their capability of producing higher actuation force than electrostatic comb drive. To find out the fracture toughness of polysilicon for these bend specimen, a bent beam actuator, as shown in Figure C.1 (a), was designed to create the failure force, F_c and deformation, δ_c at the opposite edge of a notch in the center notch bend specimens as shown in .

The failure force and critical deformation before fracture were determined by the following expressions. The value of critical fracture toughness and Young modulus of polysilicon, assumed for these calculations, were 0.7 MPam$^{1/2}$ and 169 GPa, respectively.

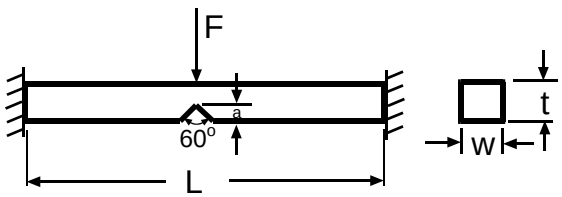

Figure C.2 Schematic view of a center notch double-clamped bend specimen

$$F_c = \frac{4 \times K_{IC} \times tw^2}{3 \times L \times \sqrt{\pi a} \times f\left(a/w\right)} \qquad (12)$$

and

$$\delta_c = \frac{F_c \times L^3}{16 \times E \times t \times w^3} \qquad (13)$$

In Eq. (12), the shape function can be found from the following equation [1]:

$$f\left(a/w\right) = 1.93 - 3.07\left(a/w\right)^2 + 14.53\left(a/w\right)^3 - 25.11\left(a/w\right)^3 + 25.8\left(a/w\right)^4 \qquad (14)$$

To find the fracture toughness of polysilicon V shape notch specimen, the same kind of thermal actuator was designed to create the failure force, F_c and deformation, δ_c. Whereas to find out fracture toughness of polysilicon of U shape notch specimen, a simple thermal actuator, as shown in C.1 (b) was designed to create F_c and δ_c. The schematic views of the specimens are shown in Figure C3 (a) & (b). The failure force and critical deformation before fracture were determined by the following expressions.

$$F_c = \frac{K_{IC} \times tw^2}{6 \times L \times \sqrt{\pi a} \times f\left(a/w\right)} \qquad (15)$$

and

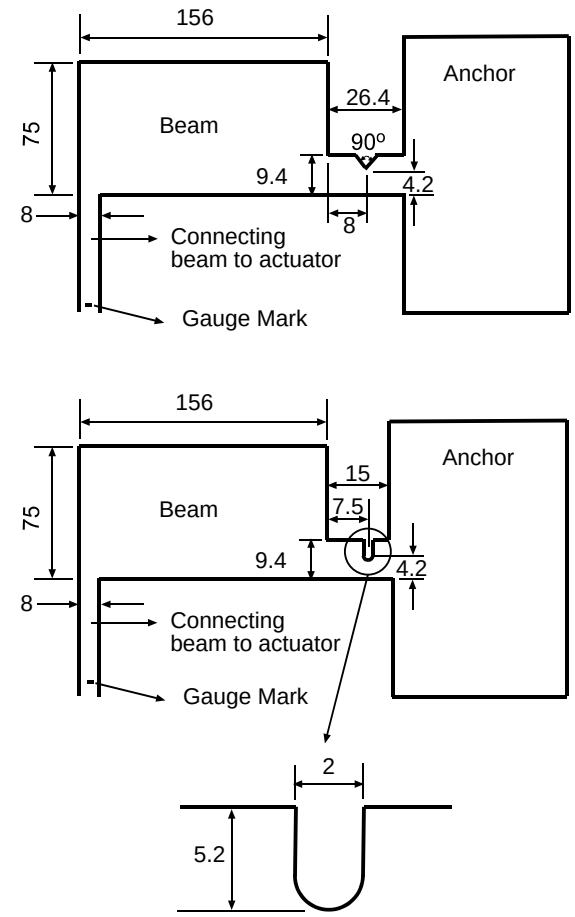

Figure C.3 Schematic view of fracture micro-specimen: (a) SENT and (b) DENT.

$$\delta_c = \frac{4 \times F_c \times L^3}{E \times t \times w^3} \qquad (16)$$

Analytical models FOR FRACTURE property:

The fracture toughness of the notch specimens can be found by measuring the fracture load. This load causes propagation of a crack at the tip of the notch specimen. The fracture toughness can be found using the following expression [**1, 8**]:

$$K_{IC} = \sigma_{\max} \sqrt{\pi a}\, f\left(a/w\right) \qquad (17)$$

where σ_{max} is the maximum stress at the notch tip due to fracture load. The maximum stress due to fracture load for fixed-fixed center notch specimen can be found by the following expression:

$$\sigma_{\max}\big|_{CN} = \frac{3FL}{2tw^2} \qquad (18)$$

The maximum stress due to fracture load for cantilever end notch specimen of shapes V or U can be found by the following expression:

$$\sigma_{\max}\Big|_{EN} = \frac{6FL}{tw^2} \qquad (19)$$

SUMMiT V model:

Figure C.4 shows a SUMMIT V design of a double-clamped center notch specimen. Geometric dimension of this specimen is shown in Table 7.

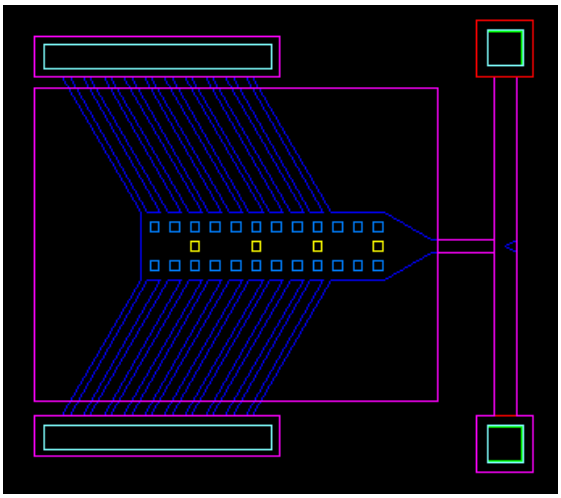

Figure C.4 SUMMIT V design of test structure for the double-clamped center notch specimen.

Table 7 Geometric dimension of double-clamped center notch specimen

Geometric Dimension		Values (μm)
Beam Length, *L*	=	300
Width of the specimen, *w*	=	20
Thickness of the specimen, *t*	=	2.25
Crack length, *a*	=	10

In this system, the actuator is modeled on the poly 3. The central part of the actuator had Poly 3 cuts for the uniform removal of sac-ox 3 from underneath. Four dimple cuts were also provided at the central structure of the actuator to prevent it from snapping down on the substrate. The actuator was anchored to the substrate on two ends, by depositing layers of poly 0, 1, 2, 3 and having them connected by providing sac-ox 1, 3 cuts. The specimen to be tested was in poly 3 and anchored to the substrate at two ends. The actuator is connected to the center of the specimen by a beam in poly 3, so that the force produced by the actuator is transferred to the center of the specimen.

Figure C.5 shows SUMMiT V design of V notched bend specimen. Geometric dimension of this specimen is shown in Table 8.

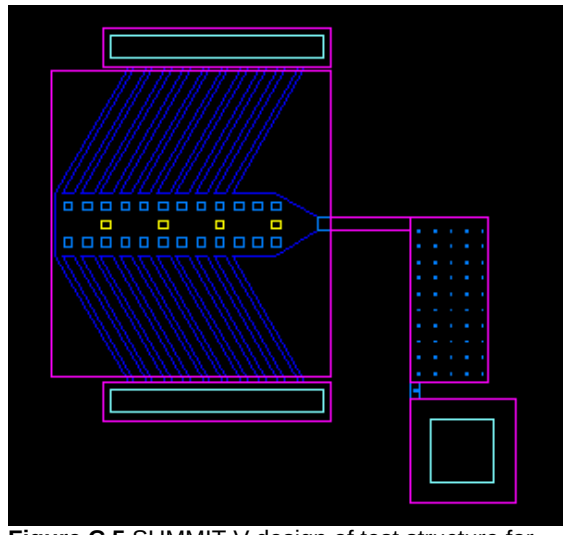

Figure C.5 SUMMIT V design of test structure for the V notched bend specimen.

Table 8 Geometric dimension of V notch bend specimen

Geometric Dimension		Values (μm)
Beam Length, *L*	=	169
Width of the specimen, *w*	=	9.4
Thickness of the specimen, *t*	=	2.25
Crack length, *a*	=	5.2

To realize this system in SUMMiT V we have the actuator on the poly 3. The central part of the actuator has Poly 3 cuts for the uniform removal of sac-ox 3 from underneath. Four dimple cuts are also provided at the central structure of the actuator to prevent it from snapping down on the substrate. The actuator is anchored to the substrate at two ends, by depositing layers of poly 0, 1, 2, 3 and having them connected by providing sac-ox 1, 3 cuts. The specimen to be tested is in poly 3 with Poly 3 cuts for uniform removal of sac-ox from beneath and anchored to the substrate at one end. The actuator is connected to one end of the specimen by a beam in poly 3, so that the force produced by the actuator is transferred to the specimen.

Figure C.6 shows SUMMiT V design of V notched bend specimen. Geometric dimension of this specimen is shown in **Error! Reference source not found.**.

Geometric Dimension		Values (μm)
Beam Length, *L*	=	163
Width of the specimen, *w*	=	9.4
Thickness of the specimen, *t*	=	2.25
Crack length, *a*	=	5.2

This design is a variant of the one in which we used the bent beam actuator. This design uses the hot arm-cold arm electro-thermal actuator. The actuator is made in the poly 2 layer and anchored to the substrate at one end with separate anchors for hot & cold arm. Array of this actuator is created and these are joined to a central beam in poly 3 through a sac-ox cut. This central beam

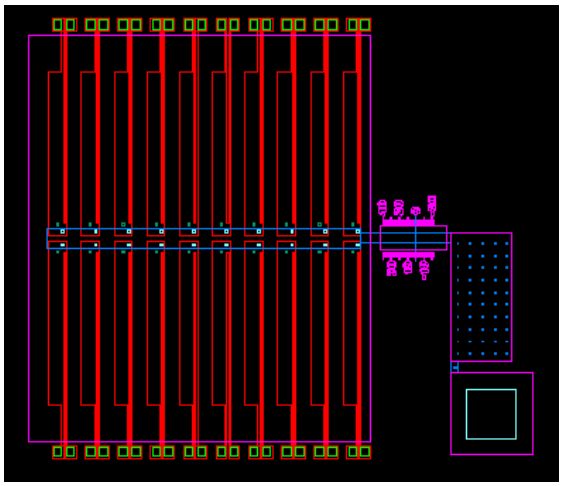

Figure C.6 SUMMiT V design of test structure for U notch bend specimen.

is used for the transfer of force from the actuator to the specimen. The specimen is in Poly 3. The specimen is provided with sac-ox 3 cuts for the uniform removal of sac-ox from underneath of the specimen. The specimen is anchored to the substrate at one end.

Expected Results:

Analytical

Table 9 Approximate analytical results for fixed-fixed center notch specimen

Fracture Strength	Required Electrostatic Force, N	Young Modulus	Deflection (μm)
K_{IC}	F_c	E	δ_c
7.00E+05	9.83E-04	1.69E+11	5.46E-07

Table 10 Approximate analytical results for V notch cantilever specimen

Fracture Strength	Required Electrostatic Force, N	Young Modulus	Deflection (μm)
K_{IC}	F_c	E	δ_c
7.00E+05	6.14E-05	1.69E+11	3.77E-06

Table 11 Approximate analytical results for U notch cantilever specimen

Fracture Strength	Required Electrostatic Force, N	Young Modulus	Deflection (μm)
K_{IC}	F_c	E	δ_c
7.00E+05	1.24E-05	1.69E+11	6.79E-07

Multiphysics

An ANSYS simulation of the bent beam actuator shown in Figures C7 and C8.

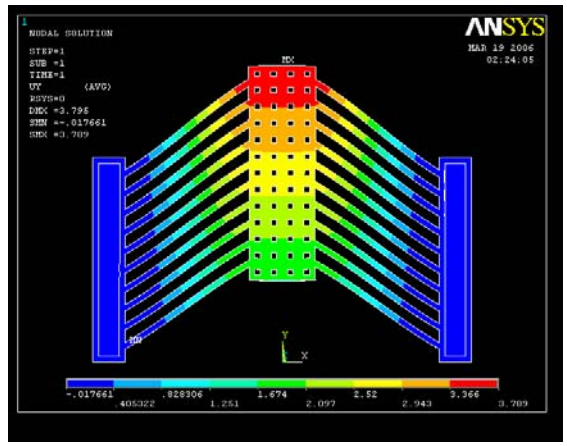

Figure C.7 ANSYS simulation of bent beam actuator

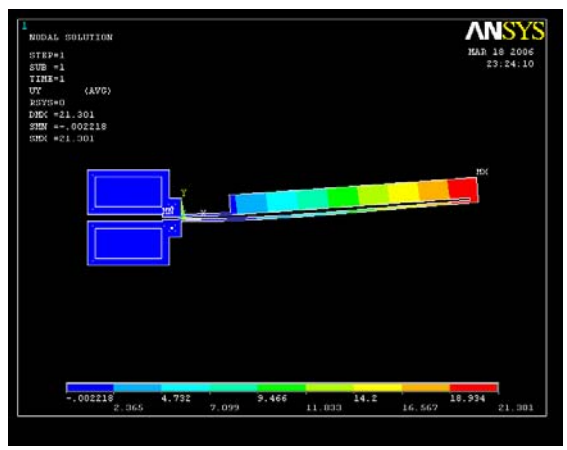

Figure C.8 ANSYS simulation of thermal actuator

Applications

1. This *in situ* test configuration can successfully measure fracture strength of a bend specimen.
2. Failure forces for the specimen can be achievable with the help of the designed actuator.

REFERENCES:

[1] **Lee, S.H., Kim, J.S., Evans, J.W., Son, D., Pak, Y.E., Jeon, J.U. and Kwon, D.** Evaluation of microfracture toughness and microcracking with notch tip radius of si film structure for microactuator in hard disk drives. *Microsystem Technologies*, 2001, **7**(3), 91-98.

[2] **Oropeza, C., Lian, K. and Wang, W.** Fracture toughness study on liga fabricated microstructures. In *Reliability, Testing, and Characterization of MEMS/MOEMS II, Jan 27-29 2003*, San Jose, CA, United States, 2003, pp. 183-191 (The International Society for Optical Engineering).

[3] **Kahn, H., Ballarini, R., Mullen, R.L. and Heuer, A.H.** Electrostatically actuated failure of microfabricated polysilicon fracture mechanics specimens. *Proceedings of the Royal Society of London Series a-Mathematical Physical and Engineering Sciences*, 1999, **455**(1990), 3807-3823.

[4] **Zhu, Y., Corigliano, A. and Espinosa, H.D.** A thermal actuator for nanoscale in situ microscopy testing: Design and

characterization. *J. Micromech. Microeng.*, 2006, **16**(2), 242-253.
[5] **Mankame, N.D. and Ananthasuresh, G.K.** Comprehensive thermal modelling and characterization of an electro-thermal-compliant microactuator. *J. Micromech. Microeng.*, 2001, **11**(5), 452-462.
[6] **Sinclair, M.J.** High force low area mems thermal actuator. *7th Intersociety Conference on Thermal and Thermomechanical Phenomena in Electronic Systems-ITherm 2000, May 23-May 26 2000 Thermomechanical Phenomena in Electronic Systems -Proceedings of the Intersociety Conference*, 2000, **1**, 127-132.
[7] **Conant, R.A. and Muller, R.S.** Cyclic fatigue testing of surface-micromachined thermal actuators. In *Proceedings of the 1998 ASME International Mechanical Engineering Congress and Exposition, Nov 15-20 1998*, Anaheim, CA, USA, 1998, pp. 273-277 (ASME, Fairfield, NJ, USA).
[8] **Gomez, F.J. and Elices, M.** A fracture criterion for blunted v-notched samples. *Int. J. Fracture*, 2004, **127**(3), 239-264.

D. MECHANICAL CHARACTERIZATION OF BIOCELL

Objectives:

The objective of this study is to explore the feasibility of designing an in situ test platform to study the characteristics of biological cells and tissues. The work is divided into two parts: (1) to build a device using SUMMIT V process and (2) to characterize the biological cells and tissues using it.

Test device configuration:

The test device consists of three components: (1) high performance comb drive, (2) connecting beam, and (3) a reservoir to hold the biological specimens. The purpose of this test structure is to measure the elastic properties of the bio-specimens [1]. A gauge is provided in the test setup to precisely measure the elongation in the specimen in response to the applied load. The high performance comb drive was used that has the capability to produce force in the range of pico-Newton to few hundred's of micro-Newton's, and a displacement in the range of 4-5 microns. A similar proposal was presented by Bronson *et al*.[2].

Working Principle:

Electrostatic comb drives are actuators where two inter-digitized comb structures can be moved together or apart by applying voltage to either of the two comb electrodes. On the application of the voltage the movable arm moves close to the fixed arm and therefore produces in-plane motion. The force from the high performance comb drive is transferred to the movable plate through a beam connected to one end of the comb drive actuator. The force produced by the actuator induces a tensile loading of the bio specimen placed in the reservoir between two plates: one is fixed and the other is connected with the actuator through a connecting beam as presented by Bronson *et al*.[2]. The study of the biological specimen under-varying load would be done on an interferometric microscope.

Figure D1 shows the SUMMiT V model for the Bio-cell characterization system. The actuator used in this design is a high performance comb drives that is one of the Sandia's standard actuators. Muthuswamy *et al*. uses similar kinds electrostatic actuators for the precise

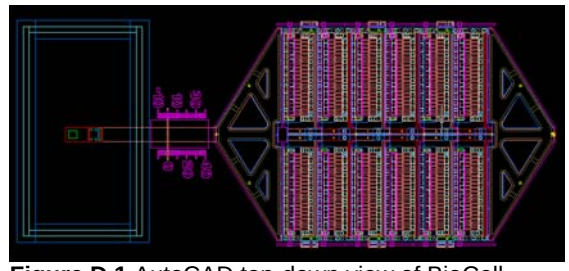

Figure D.1 AutoCAD top-down view of BioCell System.

bi-directional movement of microelectrode [3]. This actuator uses poly 0 to ploy 4 layers. The actuator is connected to the movable plated through a beam in poly 4. This beam is in turn connected to the movable plates in poly 2 through poly 3. Dimple cuts are provided underneath the movable plates to minimize its contact with the substrate. The model also has a reservoir that will hold the biological specimens to be tested. The reservoir is made by creating a wall like structure containing poly 0 to poly 3. A fixed plate is modeled inside this reservoir on poly 2. This fixed played is anchored to the substrate through sac-ox 1 cut.

DEVICE DESIGN:

DNA molecule is considered as the sample bio-cell specimen for the selection of actuator. The spring constant, *K* of DNA molecule is experimentally found to be about 10^{-8} – 10^{-7} Nm^{-1} [4]. For an assumed extension length, δ, of 12.28 μm, an approximate theoretical value of the DNA stretching force, *F*, can be found out from following expression:

$$F = K\delta \qquad (20)$$

Table 12 shows the required electrostatic force of the comb drive for this DNA stretching.

Table 12 Required electrostatic force

Spring Constant (N/m^{-1})	Deformation (μm)	Force (N)
K	δ	F
1.00E-07	1.23E-05	1.23E-12

REFERENCES:

[1] Wang, X., Li, X. and Yost, M.J. Microtensile testing of collagen fibril for cardiovascular tissue engineering. *Journal of Biomedical Materials Research - Part A*, 2005, 74(2), 263-268.
[2] Bronson, J.R., Wiens, G.J. and Tran-Son-Tay, R. A feasibility study on mems test-structures for analysis of biological. In *Proceeding of 2004 Florida Conference on Recent Advances in Robotics*, University of Central Florida in Orlando, Florida, 2004.
[3] Muthuswamy, J., Okandan, M., Jain, T. and Gilletti, A. Electrostatic microactuators for precise positioning of neural microelectrodes. *IEEE Transactions on Biomedical Engineering*, 2005, 52(10), 1748-1755.

[4] Chiou, C.H. and Lee, G.B. A micromachined DNA manipulation platform for the stretching and rotation of a single DNA molecule. *Journal of Micromechanics and Microengineering*, 2005, 15(1), 109-117.

2. NOTES

DRC Errors: DRC errors were generated in the numeral 4 in all the Sandia gauges.

DRC Advisories: Numerous P1 without P0 were generated by poly1 bridges over poly0 traces. Numerous bond pad related advisories also occurred.